

## SYNTHESIS, CHARACTERIZATION AND PHOTOCATALYTIC APPLICATIONS OF S-DOPED GRAPHITIC CARBON NITRIDE NANOCOMPOSITES WITH NICKEL DOPED ZINC OXIDE NANOPARTICLES

M. JAVED<sup>a</sup>, M. A. ABID<sup>b</sup>, S. HUSSAIN<sup>c\*</sup>, D. SHAHWAR<sup>a</sup>, S. ARSHAD<sup>a</sup>,  
N. AHMAD<sup>a</sup>, M. ARIF<sup>a</sup>, H. KHAN<sup>a</sup>, S. NADEEM<sup>a</sup>, H. RAZA<sup>a</sup>, S.M. HARRON<sup>a</sup>

<sup>a</sup>*Department of chemistry, School of Science, University of Management and Technology, Lahore, Pakistan*

<sup>b</sup>*Department of Chemistry, University of Sahiwal, Sahiwal, Pakistan*

<sup>c</sup>*Department of Chemistry, Lahore Garrison University, DHA Phase VI, Lahore, Pakistan*

Coprecipitation method was adopted for the synthesis of undoped and Ni-doped zinc oxide nanoparticles. The photocatalytic activity of the synthesized particles was examined by degradation of methylene blue under UV bulb. The S-doped graphitic carbon nitride was obtained by calcination of thiourea and composites were formed with S-doped graphitic carbon nitride and nickel doped zinc oxide nanoparticles using liquid exfoliation method. The ethanol and water were used as solvents for the liquid exfoliation. The photocatalytic activity was performed under UV and visible light by using a UV-visible spectrophotometer with different concentrations of composites for the degradation of methylene blue. The doping of nickel on zinc oxide nanoparticles and formation of sulfur doped graphitic carbon nitride composites were confirmed by FTIR and XRD analyses. The FTIR analysis showed a signal at  $838\text{cm}^{-1}$  due to the presence of Ni-O bond. The peaks at  $3649\text{cm}^{-1}$  and  $3735\text{cm}^{-1}$  confirmed the presence of amide group. The shift in absorption maxima from 364nm to 376nm (red shift) in UV spectrum was a confirmation of increased Ni content. The different concentrations of composites showed great impact on the degradation of methylene blue.

(Received March 11, 2020; Accepted October 28, 2020)

**Keywords:** Photocatalytic, Nanocomposites, S-doped graphitic carbon nitride, Ni-doped ZnO

### 1. Introduction

The nano-materials show outstanding physical, chemical and biological characteristics as compared to their bulk counterparts and have gained prominence in technological advancements [1-3]. The chemical stability, thermal stability and greater mechanical strength make the ZnO better oxide as compared all other nanostructures. ZnO nano-materials have unique electrical, mechanical and optical properties and find applications in field emission, gas sensors, nano ultraviolet lasers and photocatalysts [4]. They have attracted greater attention in the field of photovoltaic, photocatalytic activity and electronics due to better mechanical strength, improved stability and enhanced electron flow [5]. Zinc oxide among all the photocatalysts shows unique characteristics, like enhanced oxidation-reduction potentials, cheaper, nontoxic and safe for the environment. The selection of proper or suitable photocatalyst depends on the better light absorption ability and stimulates redox reactions. Zinc oxide photocatalyst revealed higher photocatalytic degradation power to pollutants as compared to  $\text{TiO}_2$  by absorbing greater amount of UV spectrum and has  $200\text{-}300\text{cm}^2\text{V}^{-1}\text{S}^{-1}$  electron flow or mobility. Zinc Oxide has broad band gap 3.37 eV and undoped zinc oxide showed n-type conductivity [6]. Doping the ZnO nanoparticles with a metal may enhance the charge separation ability and increase the generation of OH radicals which leads to increased degradation of organic pollutants. By introducing impurities in the ZnO lattice, the physical and chemical characteristics will improve through shifting valence bond energy of ZnO up and band gap energy becomes narrower to the UV-visible

region [5]. For example optical properties and photocatalytic activity can be enhanced by the Ni-doping on ZnO nanoparticles [7].

Graphitic carbon nitride ( $g\text{-C}_3\text{N}_4$ ) is polymeric semiconductor; its attractive electronic structure of tri-s-triazine ring and greater condensation degree make the polymer highly stable against chemical and thermal effects with medium band gap. The separation of photo generated electron-hole pairs is possible when valence band and conduction band levels are perfectly matched [8]. Doping of  $g\text{-C}_3\text{N}_4$  matrix with various inorganic, organic metals or compounds can improve its properties e.g. dye adsorption and light absorption etc [9]. Non-metal doping on  $g\text{-C}_3\text{N}_4$  such as S results in decrease of band gap and light absorption ability [10]. Due to S-doping, the  $g\text{-C}_3\text{N}_4$  behaves like a conductor. The non-uniform distribution of S-over  $g\text{-C}_3\text{N}_4$  collect excited electrons and undoped areas behaves like a photo anode. The whole scenario promotes charge separation and increased photocatalytic activity. S-doping appeared outstanding changes in the electronic structure of  $g\text{-C}_3\text{N}_4$ , doping causing narrower the band gap and converted the material into a conductor [11]. As far as chemistry of sulfur doping is concerned, length of S-C bond (1.75Å) is larger than that of original C-N bond (1.35Å). Band gap of S-doped  $\text{C}_3\text{N}_4$  sheet is 0.20 eV much smaller than pristine  $\text{C}_3\text{N}_4$  -2.70eV thus could allow more efficient charge transfer due to different electronegativity between S and N bonds [12].

Thiourea has self-ability of polymerization and condensation at high temperature and forms sulfur doped graphite carbon nitride in which sulfur sites promote the connectivity and packing of  $g\text{-C}_3\text{N}_4$  sheets because sulfur gave stronger chemical control for the synthesis of  $g\text{-C}_3\text{N}_4$  networks and promoting the process of  $g\text{-C}_3\text{N}_4$  polymerization and condensation. The high temperature of about 650°C is suitable for the synthesis of S-doped graphite carbon nitride [13].

Solar irradiation decomposes the water pollutants into less harmful compounds during the photo catalytic degradation. Various photo catalysts like  $\text{TiO}_2$  have been used in industrial applications for the degradation of dyes. For the better and improved charge separation and electron transfer process the combination of  $g\text{-C}_3\text{N}_4$  and CuO established the hetero-structure which showed improved visible light driven photocatalytic activities [14]. Heterojunction is a method to enhance photocatalytic activity with extended carrier life time and improved charge transfer of interfacial interactions [13, 15]. Current studies were carried out for designing a nanocomposite for having combined properties of  $g\text{-C}_3\text{N}_4$  and ZnO, co-precipitation method was adopted for fabrication and analyzed for respective treatments.

## 2. Experimental

### 2.1. Chemicals and instruments

All the chemicals and reagents of analytical grade were utilized in the current study. Zinc acetate, nickel nitrate, and polyvinylpyrrolidone (PVP) were of Unichem origin. Sodium hydroxide and thiourea were purchased from Sigma-Aldrich. Methylene blue was procured from BDH England. Solvents used were also purchased of analytical grade quality. For the studies of analyte concentrations on absorbance and transmittance UV-visible JASCO V-770 spectrophotometer with wavelength up to 800nm was used. The crystal structure of undoped and nickel doped zinc oxide nanoparticles and sulfur doped graphitic carbon nitride were studied by X-PERT PRO PAN analytical diffractometer with source of  $\text{CuK}\alpha$  ( $\lambda = 1.5419 \text{ \AA}$ ), voltage 40kV and a current 40 mA. The analytical instrument Bruker Diamond IR spectrometer was used for the studies of chemical structure and vibration states to identify the chemical bonds present between molecules.

### 2.2. Synthesis of composites

#### 2.2.1 Synthesis of ZnO nanoparticles

Undoped ZnO nanorods were synthesized by coprecipitation method using zinc acetate dehydrate. Zinc acetate (0.1g) and PVP (3g) were dissolved in 100 mL deionized water followed by drop wise addition of 10M NaOH (10mL). White precipitates appeared on addition of NaOH which were filtered and washed with ethanol repeatedly and oven dried at 80°C for 4 hours.

Sample was then calcined in furnace for 2 hours at 550 °C. The white powder of un-doped zinc oxide was obtained and finely ground for further use.

### **2.2.2. Synthesis of Ni doped ZnO nanoparticles**

Coprecipitation method was adapted for formation of Ni doped ZnO nanoparticles with different concentrations of nickel (0.03, 0.06 and 0.09 M). Nickel nitrate (0.2g), zinc acetate dehydrate (1.8g) and PVP (3g) were dissolved in 100 mL deionized water and 10 mL of NaOH was added drop wise. Precipitates were filtered, washed with ethanol and dried in oven at 80 °C for 4 hours. Finally, the calcination of samples was carried out at 550°C for 2 hours and ground into fine powder. Variable compositions were prepared depending on doping ratio of nickel in grey color.

### **2.2.3. Synthesis of S-doped – g-C<sub>3</sub>N<sub>4</sub>**

Thiourea was heated at 650°C for 2 hours in furnace. After that, the dried S-doped yellow powder was collected and ground in pestle and mortar.

## **2.3. Liquid exfoliation**

### **2.3.1 Preparation of composites using ethanol as a solvent**

0.1g of nickel doped zinc oxide nanoparticles and 0.1g of S-doped g-C<sub>3</sub>N<sub>4</sub> were dissolved in 25mL of ethanol each. Each solution was mechanically stirred with glass rod for 30 minutes. Both solutions were mixed followed by well mixing and then suspension was placed in dark under magnetic stirring for 30 minutes to achieve adsorption equilibrium. The suspension was centrifuged for 10 minutes and filtered. Filtrate was then mixed well in acetone and dried at 60°C for 3 to 4 hours. The S-doped-g-C<sub>3</sub>N<sub>4</sub> with Ni doped zinc oxide composites were prepared by this method with different concentrations of nickel doping (0.1, 0.2, 0.3, 0.4M).

### **2.3.2. Preparation of methylene blue (MB) solution**

Methylene blue solution (0.3x10<sup>-3</sup>M) was prepared by dissolving 0.01g of MB powder in 100mL of water.

### **2.3.3. Photocatalytic activity**

Photocatalytic activity of composites was examined by the degradation of methylene blue. The 0.3x10<sup>-3</sup>M MB solution was prepared and 10mg of composite (catalyst) was added to the dye solution. The solution mixture was placed in dark for 30 minutes with continuous stirring and adsorption equilibrium was achieved by homogeneous dispersion of solution. The solution was placed under UV- light with constant stirring and 5 mL of solution was taken out and rotated in a centrifuge at 4000 rpm for 5 minutes. The residual was separated out and filtrate was obtained. The UV visible spectrophotometer was used to examine the degradation of methylene blue. Deionized water and filtrate were filled in the cuvettes and the absorption spectra were recorded. Change in absorption intensity was examined due to degradation of methylene blue.

### **2.3.4. Preparation of composites using water as a solvent**

For the preparation of composites, first of all 0.1g of sulfur doped g-C<sub>3</sub>N<sub>4</sub> was dissolved in 25 mL water and 0.06g of nickel doped ZnO nanoparticles were dissolved in 25 mL water separately. Then both solutions were mixed well under continuous stirring. Afterwards, the suspension was placed in dark with constant stirring for 30 minutes to achieve adsorption equilibrium.

### **2.3.5. Photocatalytic activity**

After that 0.3x10<sup>-3</sup>M MB solution was added in the suspension and placed on magnetic stirrer in visible light. In the next step 5 mL of solution was taken out and rotated in centrifuge for 3 to 5 minutes. The filtrate was obtained to investigate the degradation of the methylene blue using UV spectrophotometer. Same method was repeated for other concentrations.

### 3. Results and discussions

Successful synthesis and applications of the composite formed was characterized using spectroscopic and morphological analyses techniques.

#### 3.1.X –ray diffraction studies

XRD is very informative technique for the analysis of structure of compound, its crystallite size and impurities present in the matrix [16]. This technique was also useful for the determination of change in crystal size and phase morphology of synthesized nanomaterials and doping effect on them [17]. All peak values were indexed to the diffractions of (100), (002), (101), (102), (110), (103), (200), (112), (201), (004), (202) planes and showed exact hexagonal wurtzite structure of ZnO nanoparticles. Figure 1 displays XRD spectra for undoped ZnO nanoparticles, nickel doped ZnO nanoparticles, sulfur doped graphitic carbon nitride, S-doped g-carbon nitride with nickel doped ZnO Composite and S-doped-g-carbon nitride with nickel doped ZnO Composite.

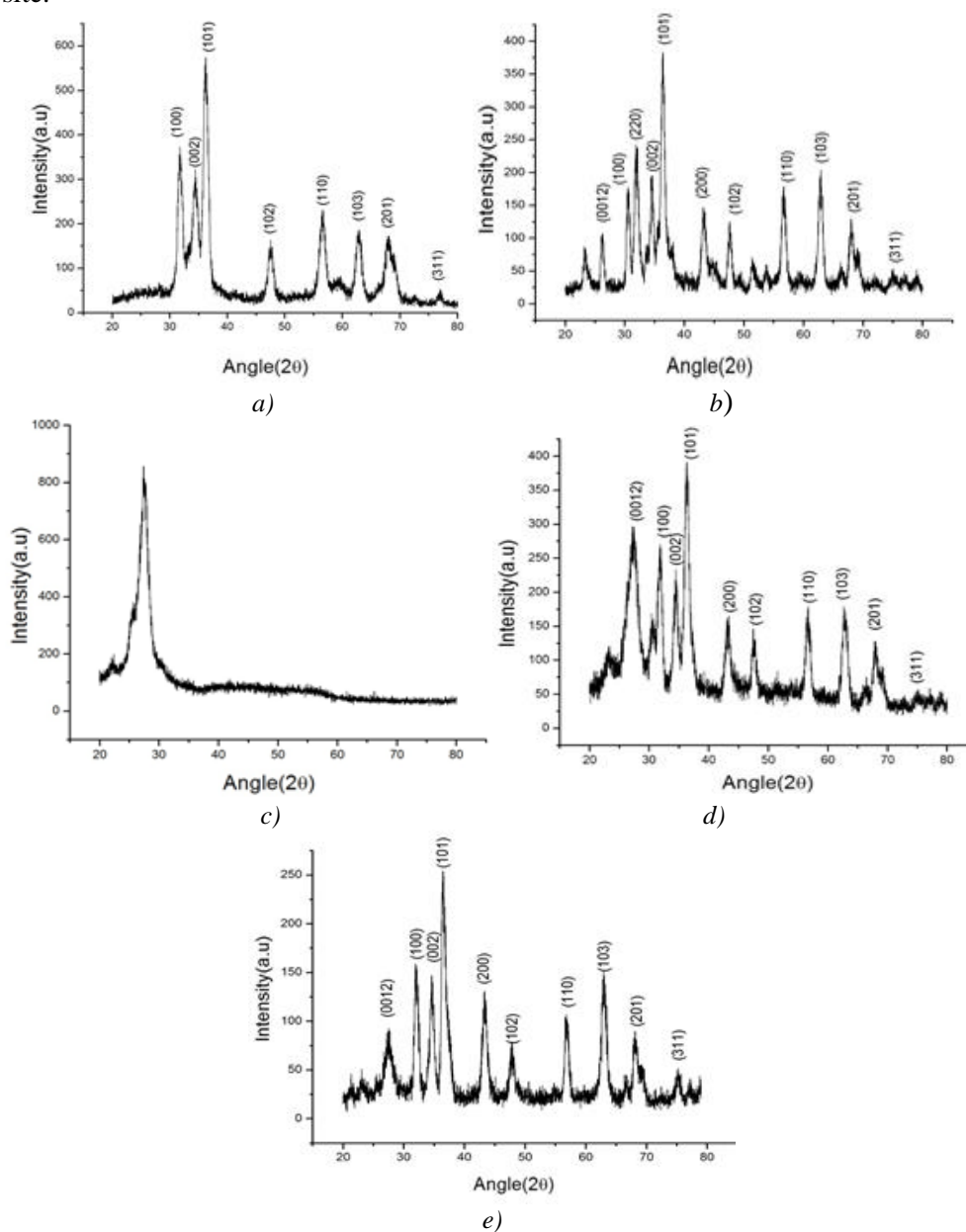


Fig. 1. XRD spectra for (A) undoped ZnO nanoparticles (B) nickel doped ZnO nanoparticles (C) sulfur doped graphitic carbon nitride (D) S-doped g-carbon nitride with nickel doped ZnO Composite (E) S-doped-g-carbon nitride with nickel doped ZnO Composite.

On Nidoping with different concentrations lower the intensity of the peak and reduces the crystallite size of undoped zinc oxide [18]. The peak at (002) plane showed the presence of sulfur doped g-carbon nitride on nickel doped zinc oxide nanoparticles. Peak broadening and reduced crystallite size has also been noticed owed to increased Ni proportion in the designed composites. Layered structure of S-g-C<sub>3</sub>N<sub>4</sub> was examined which showed peak at (002) and lower intensity of diffraction peak because of doping of Sulphur [19]. XRD patterns also confirmed the structural insight to the composite, upon increasing the nickel doped zinc oxide concentrations on the sulfur doped g-carbon nitride; decrease in crystallinity may be noticed as depicted in Figure 1E.

### 3.2. FT-IR assay

FT-IR spectroscopic analysis is highly important tool for the evaluation of chemical bonds in the molecules[20, 21]. The spectral peak positions and absorption bands revealed the structure, morphology and composition of a substance [22]. Each compound has its own unique IR spectrum due to specific arrangement of atoms. Because of this property the IR spectra give correct identification of various compounds and materials[23]. At 838cm<sup>-1</sup>, weak absorption band because of Ni- O vibrational frequency revealed the presence of doped nickel in the lattice structure of ZnO which was in accordance to theoretical values, as stretching modes of metal oxides are reported in range of 400-800cm<sup>-1</sup> the unique stretching modes of metal oxides were revealed[16]. Figure 2 displays FTIR spectra for doped ZnO nanoparticles, Ni doped 0.03% ZnO nanoparticles and S-doped-g-carbon nitride with Ni doped ZnO nanoparticles.

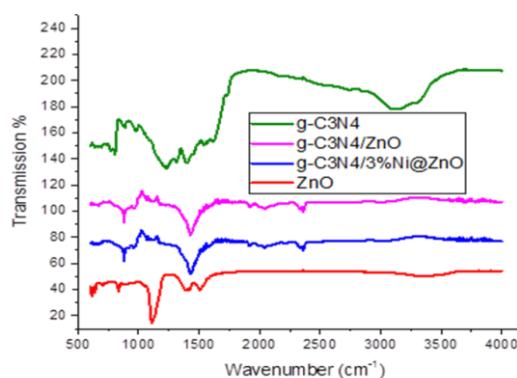


Fig. 2. FTIR spectra for S-doped-g-carbon nitride, ZnO/Sulfur doped g-C<sub>3</sub>N<sub>4</sub> nanocomposite, 3% Ni doped ZnO/Sulfur doped g-C<sub>3</sub>N<sub>4</sub> nanocomposite and ZnO nanoparticles.

S-doped g-C<sub>3</sub>N<sub>4</sub> was also investigated through FTIR analysis, the spectrum showed signals at 1541cm<sup>-1</sup> and 1396cm<sup>-1</sup> in agreement to stretching vibration modes of heptazine heterocyclic ring (C<sub>6</sub>N<sub>7</sub>) units. The peak value at 838 cm<sup>-1</sup> showed breathing mode of triazine units correlated to condensed C-N heterocycles. The absorption of CO<sub>2</sub> from atmosphere assigned at 2360 cm<sup>-1</sup>. No peak was observed for S owed to its minimal amount present. The region at 1396cm<sup>-1</sup> showed a strong absorption signal due to bending mode of hydroxyl group. The stretching band of O-H group at 3649 to 3735 cm<sup>-1</sup> was also noted, Figure 2C in addition to signals at 2900 cm<sup>-1</sup> and 3500 cm<sup>-1</sup> characteristic of adsorbed H<sub>2</sub>O molecules and N-H vibrations of uncondensed amino groups, respectively[19]. The absorption region around 3800cm<sup>-1</sup> to 2700 cm<sup>-1</sup> confirmed the presence of C-H, O-H and N-H bonds and the amide group displayed zero to two N-H absorption bands at 3735cm<sup>-1</sup>.

### 3.3. UV-visible assay

UV-visible spectroscopy revealed the substitution of nickel doping on the zinc oxide structure. The undoped zinc oxide showed its absorption band at the range of 364nm and after nickel doping the absorption maxima shifted to 374nm and 376nm, showed red shift. The red shift

due to nickel doping revealed the confirmation of nickel ions properly incorporated into zinc oxide structure [24]. Figure 3 displays UV visible spectra of undoped ZnO and Ni-doped zinc oxide.

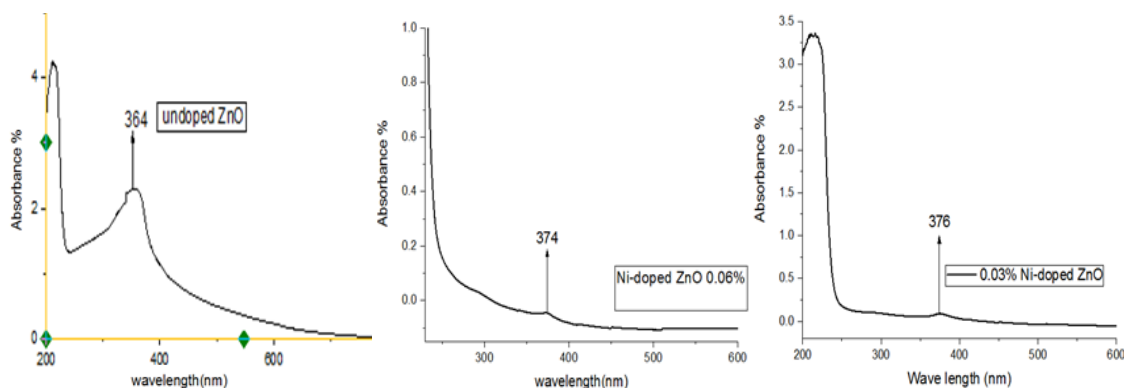


Fig. 3. UV visible spectra of undoped ZnO and Ni-doped zinc oxide.

As nickel ions substituted zinc ions, the localized d electrons and band electrons interacted and exchanged within the sp-d orbitals causing red shift in dopant samples. Because of red shift the band gap and band edge were decreased [25]. The absorption intensity was increased due to nickel doping [26]. The photocatalytic activity of undoped zinc oxide nanoparticles was examined by the degradation of methylene blue dye. Undoped zinc oxide nanoparticles showed more than 50% of degradation after 25 minutes under UV. The degradation of MB was observed due to oxygen vacancies and zinc atom. Methylene blue gained electrons from excited states of zinc oxide and decomposed. Figure 4 displays UV-visible spectra for undoped ZnO nanoparticles, 0.03% Ni doped ZnO nanoparticles and 0.03% Ni doped ZnO nanoparticles for the degradation of MB.

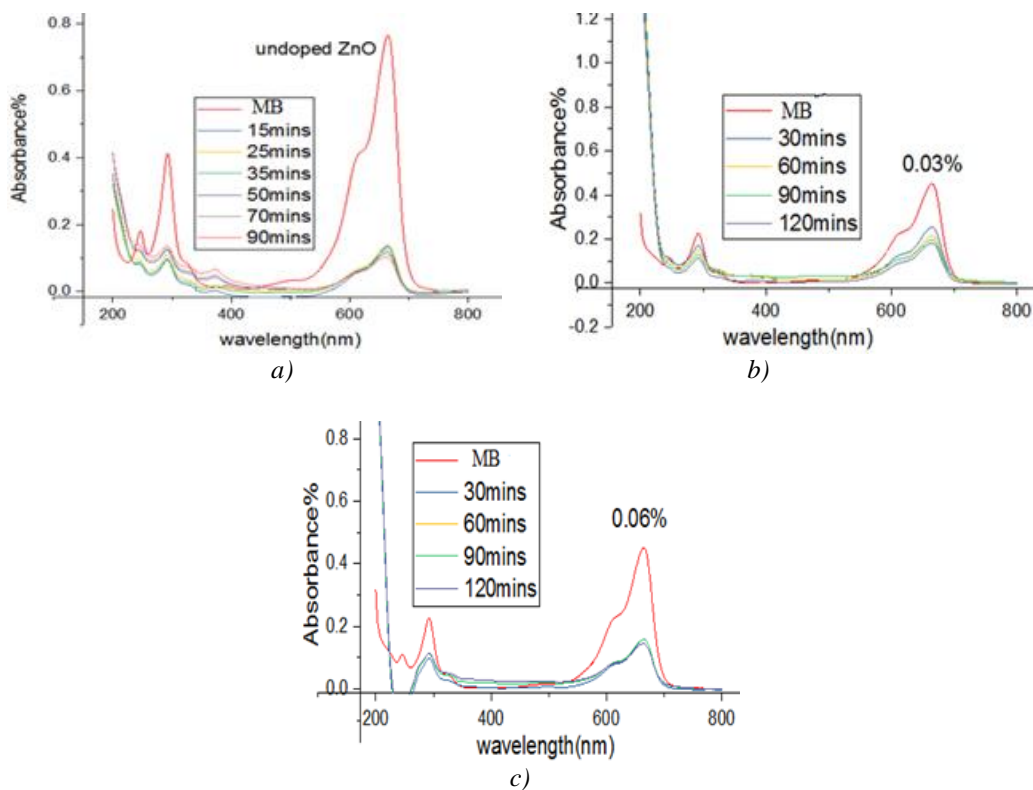


Fig. 4. UV-visible spectra for (A) undoped ZnO nanoparticles (B) 0.03% Ni doped ZnO nanoparticles (C) 0.06% Ni doped ZnO nanoparticles for the degradation of MB.

The photocatalytic activity of 0.03M nickel doped zinc oxide nanoparticles showed better degradation of MB as compared to 0.06 and 0.09M samples (Figure 5). The slower degradation of MB in doped samples is caused by fast recombination of electron hole pairs [27].

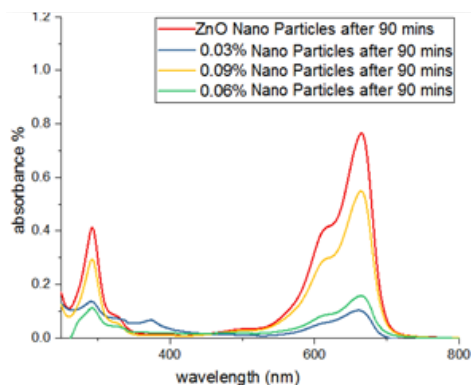


Fig. 5. UV-visible spectra of undoped ZnO and nickel doped ZnO with different concentrations.

### 3.4. Photocatalytic activity

Figure 6 displays UV-visible spectra of composites prepared in ethanol and water

#### 3.4.1. Ethanol used as a solvent

In Figure 6, the degradation of MB is greater in pure ZnO nanoparticles whereas in 0.03% sample MB showed better degradation than other dopant concentrations. The degradation of dye not only depends upon proper amount of concentration of doping but also on size reduction. For the degradation of MB the decreased photocatalytic activity of Ni-doped ZnO is due to defects developed by doping which can reduce the recombination of electron hole pairs. Same effect was observed on the degradation of MB when composites were used.

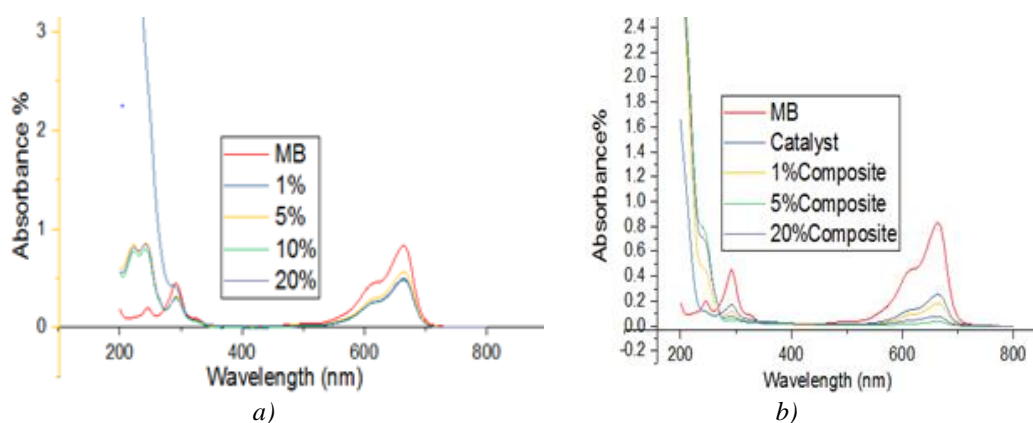


Fig. 6. UV-visible spectra of composites prepared in (A) ethanol and (B) water.

#### 3.4.2 Water used as a solvent

The degradation of MB with different concentrations of sulfur doped  $g\text{-C}_3\text{N}_4$  with the nickel doped ZnO showed better results specially 5% sample degraded dye in time duration of 5 minutes. Secondly, 10% sample degraded dye in 08 minutes as compared to 1% and 20% samples. All these samples degraded dye in visible light without using UV light. Liquid exfoliation is a unique way to obtain ultra-thin nanosheets of sulfur doped g-carbon nitride from bulk g-carbon

nitride to improve its surface area, efficient transport of electrons as well as to enhance its photocatalytic activity and lessen the recombination rate of charge carriers [5].

In the present work, two solvents; ethanol and water have been used for exfoliation of sulfur doped g-carbon nitride. In water ultra-thin nanosheets were prepared which were very stable in acidic as well as basic medium. These sheets showed efficient photo absorption ability. These nanosheets displayed nonhazardous and ecofriendly effects because water was used as a solvent [13]. In first method Ni-doped ZnO nanoparticles with S-doped g-C<sub>3</sub>N<sub>4</sub> composites prepared in ethanol solvent with fixed ratio of S-doped g-C<sub>3</sub>N<sub>4</sub> displayed slow photocatalytic activity because of increased amount of nickel doping which reduced the recombination of electron hole pair due to defects. Moreover, due to formation of SO<sub>3</sub> and SO<sub>4</sub> anionic species also reduced the photocatalytic degradation of dye. Whereas, in second method composites prepared in water with varying amounts of S-doped g-C<sub>3</sub>N<sub>4</sub> and the fixed Ni-doped ZnO nanoparticles showed better results in minimum time period. This all has been attributed to efficient exfoliation of S-doped g-C<sub>3</sub>N<sub>4</sub> sheets in water with Ni-doped ZnO nanoparticles which increased the active sites for more adsorption of dye molecules on its increased surface area.

#### 4. Conclusions

The undoped ZnO and nickel doped zinc oxide nanoparticles with different concentrations of nickel were prepared using coprecipitation method and their photocatalytic activity was examined with methylene blue dye. The nanoparticles displayed better photo degradation under UV light and showed better photocatalytic activity. Secondly, Sulfur doped graphitic carbon nitride was prepared by calcination of thiourea. The composites were prepared by S-doped graphite carbon nitride with undoped zinc oxide and nickel doped zinc oxide nanoparticles using liquid exfoliation method. Ethanol and water were used as solvents for exfoliation. The composites which were prepared with different concentrations of doping materials showed efficient degradation of methylene blue under UV and visible light. Thirdly, comparison of results revealed that S-doped graphitic carbon nitride with nickel doped ZnO composites displayed efficient degradation of dye in water in the presence of visible light as compared to ethanol under UV light.

#### References

- [1] J. Jeevanandam, A. Barhoum, Y. S. Chan, A. Dufresne, M. K. Danquah, *Beilstein journal of nanotechnology* **9**(1), 1050 (2018).
- [2] M. Javed, S. M. Abbas, S. Hussain, M. Siddiq, D. Han, L. Niu, *Materials Science for Energy Technologies* **1**(1), 70 (2018).
- [3] S. M. Abbas, N. Ahmad, U. Ali, S. U.-d. Khan, S. Hussain, K.-W. Nam, *Electrochimica Acta* **212**, 260 (2016).
- [4] D. Sahu, C. P. Liu, R. C. Wang, C. L. Kuo, J. L. Huang, *International Journal of Applied Ceramic Technology* **10**(5), 814 (2013).
- [5] C. B. Ong, L. Y. Ng, A. W. Mohammad, *Renewable and Sustainable Energy Reviews* **81**, 536 (2018).
- [6] N. V. Kaneva, D. T. Dimitrov, C. D. Dushkin, *Applied Surface Science* **257**(18), 8113 (2011).
- [7] K. Qi, B. Cheng, J. Yu, W. Ho, *Journal of Alloys and Compounds* **727**, 792 (2017).
- [8] Y. Wang, X. Wang, M. Antonietti, *Angewandte Chemie International Edition* **51**(1), 68 (2012).
- [9] S. Yan, Z. Li, Z. Zou, *Langmuir* **26**(6), 3894 (2010).
- [10] L. Yin, Y.-P. Yuan, S.-W. Cao, Z. Zhang, C. Xue, *Rsc Advances* **4**(12), 6127 (2014).
- [11] S. Stolbov, S. Zuluaga, *Journal of Physics: Condensed Matter* **25**(8), 085507 (2013).
- [12] Z. Pei, J. Zhao, Y. Huang, Y. Huang, M. Zhu, Z. Wang, Z. Chen, C. Zhi, *Journal of Materials Chemistry A* **4**(31), 12205 (2016).
- [13] G. Zhang, J. Zhang, M. Zhang, X. Wang, *Journal of Materials Chemistry* **22**(16), 8083 (2012).

- [14] J. Wang, H. Xu, X. Qian, Y. Dong, J. Gao, G. Qian, J. Yao, *Chemistry–An Asian Journal* **10**(6), 1276 (2015).
- [15] B. Jeong, D. H. Kim, E. J. Park, M.-G. Jeong, K.-D. Kim, H. O. Seo, Y. D. Kim, S. Uhm, *Applied Surface Science* **307**, 468 (2014).
- [16] R. Jeyachitra, N. Sriharan, V. Senthilnathan, T. Senthil, *Journal of Advances In Chemistry* **12**(6), 4097 (2016).
- [17] P. SivaKarthik, V. Thangaraj, S. Kumaresan, K. Vallalperuman, *Journal of Materials Science: Materials in Electronics* **28**(14), 10582 (2017).
- [18] S. Rana, R. P. Singh, *Journal of Materials Science: Materials in Electronics* **27**(9), 9346 (2016).
- [19] K. Wang, Q. Li, B. Liu, B. Cheng, W. Ho, J. Yu, *Applied Catalysis B: Environmental* **176**, 44 (2015).
- [20] S. Hussain, S. Ali, S. Shahzadi, M. N. Tahir, M. Shahid, *Journal of Coordination Chemistry* **68**(14), 2369 (2015).
- [21] S. Hussain, S. Ali, S. Shahzadi, S. K. Sharma, K. Qanungo, I. H. Bukhari, *Journal of Coordination Chemistry* **65**(2), (2012).
- [22] Z. Yang, Z. Ye, Z. Xu, *Physica E: Low-Dimensional Systems and Nanostructures* **42**(2), 116 (2009).
- [23] Z. A. Fattah, *International journal of Engineering Sciences and Research Technology* **2013**, 2277 (2016).
- [24] M. Gholami, M. Shirzad-Siboni, J.-K. Yang, *Korean Journal of Chemical Engineering* **33**(3), 812 (2016).
- [25] R. Elilarassi, G. Chandrasekaran, *Optoelectronics letters* **6**(1), 6 (2010).
- [26] X. Cai, Y. Cai, Y. Liu, H. Li, F. Zhang, Y. Wang, *Journal of Physics and Chemistry of Solids* **74**(9), 1196 (2013).
- [27] R. Ullah, J. Dutta, *Journal of Hazardous materials* **156**(1-3), 194 (2008).